Available online at www.sciencedirect.com
ScienceDirect
Journal of Organometallic Chemistry 692 (2007) 1099–1109
Journal of Organometallic Chemistry
www.elsevier.com/locate/jorganchem

Pentamethylcyclopentadienyl organoiron(II) hydrazone complexes: Synthesis, spectroscopic characterization, and second-order nonlinear optical properties. X-ray crystal structure of $[(\eta^5\text{-}C_5Me_5)Fe(\eta^6\text{-}C_6H_5)NHNH_2]^+PF_6^-$

Mauricio Fuentealba [a,d], Loïc Toupet [b], Carolina Manzur [a,*], David Carrillo [a,*], Isabelle Ledoux-Rak [c], Jean-René Hamon [d,*]

[a] Laboratorio de Química Inorgánica, Instituto de Química, Pontificia Universidad Católica de Valparaíso, Avenida Brasil 2950, Valparaíso, Chile
[b] UMR 6626, Groupe Matière Condensée et Matériau, CNRS-Université de Rennes 1, Campus de Beaulieu, 35042 Rennes Cedex, France
[c] Laboratoire de Photonique Quantique et Moléculaire, UMR 8537 CNRS-ENS Cachan, 61 Avenue du Président Wilson, 94235 Cachan Cedex, France
[d] UMR 6226 "Sciences Chimiques de Rennes", CNRS-Université de Rennes 1, Campus de Beaulieu, 35042 Rennes Cedex, France

Received 17 October 2006; accepted 3 November 2006
Available online 12 November 2006

Abstract

A series of novel pentamethylated sandwich complexes based on the $[Cp^*Fe(\eta^6\text{-}C_6H_5)]^+$ core ($Cp^* = \eta^5\text{-}C_5Me_5$) has been prepared. The new organometallic π-conjugated push–pull chromophores $[Cp^*Fe(\eta^6\text{-}C_6H_5)\text{-}NHN{=}CHR]^+PF_6^-$ (R = 2,4,6-$Me_3C_6H_2$, **4**; $(\eta^5\text{-}C_5H_5)Fe(\eta^5\text{-}C_5H_4)$, **5**) were prepared through condensations between the organometallic hydrazine precursor $[Cp^*Fe(\eta^6\text{-}C_6H_5NHNH_2)]^+PF_6^-$ (**3**), and either the mesitaldehyde or the ferrocenecarboxaldehyde, respectively. Their original design combines the cationic mixed sandwich acceptor (A) associated with an organic or organometallic donor (D) through the asymmetric hydrazone spacer –NH–N=CH–. The mesityl ring of **4** has been complexed by the arenophile Cp^*Ru^+, leading to the first η^6:η^6-coordinated dinucleating hydrazone complex, $[Cp^*Fe(\eta^6\text{-}C_6H_5)\text{-}NHN{=}CH\text{-}\{(\eta^6\text{-}2,4,6\text{-}Me_3C_6H_2)RuCp^*\}]^{2+}[PF_6^-]_2$ (**6**). Both the mono- and dinuclear hydrazones were stereoselectively obtained as their *trans*-isomers about the N=C double bond. All the new compounds were thoroughly characterized by a combination of elemental analysis and spectroscopic techniques (^1H and ^{13}C NMR, IR and UV–Vis). In addition, the solid-state structure of the organometallic hydrazine precursor **3** has been determined by X-ray diffraction study. Spectroscopic and electrochemical data of the organometallic hydrazones **4** and **5** clearly indicate a mutual donor–acceptor electronic influence resulting from conjugation between the end groups through the entire hydrazone backbone. Compounds **4** and **5** are strongly polarized D–π–A systems exhibiting low-lying intramolecular charge transfer bands in their electronic absorption spectra and enhanced second-order NLO properties (μβ), as measured by EFISH technique at 1.907 μm.

Keywords: Sandwich complex; Iron complex; Arenehydrazone–iron complex; Nonlinear optics; X-ray structure; Push–pull complex

1. Introduction

Metallocene and related half and mixed sandwich complexes have been at the vanguard of organometallic chemistry for over 50 years possessing a myriad of uses and applications encompassing synthetic, catalytic, medicinal, and materials science [1–3]. Among those, the cationic isolobal electron-acceptor counterpart of ferrocene, the mixed sandwich derivative $[CpFe(\eta^6\text{-arene})]^+$ ($Cp = \eta^5\text{-}C_5H_5$), have also long been of interest due to their important position in the development of metal-assisted organic synthesis [4], organometallic polymers [5], and as organometallic route to dendrimers using the $CpFe^+$ induced

* Corresponding authors. Fax: +56 32 27 34 20 (C. Manzur), fax: +56 32 27 34 20 (D. Carrillo), fax: +33 2 23 23 56 37 (J.-R. Hamon).
E-mail addresses: cmanzur@ucv.cl (C. Manzur), david.carrillo@ucv.cl (D. Carrillo), jean-rene.hamon@univ-rennes1.fr (J.-R. Hamon).

0022-328X/$ - see front matter © 2006 Elsevier B.V. All rights reserved.
doi:10.1016/j.jorganchem.2006.11.008

polyfunctionalization of polymethylbenzenes [6]. Moreover, their interesting redox properties [7] allow studies of electronic communication between ligand-bridged metals [8]. In comparison, the analogous chemistry of substituted pentamethyl counterparts $[Cp^*Fe(\eta^6\text{-arene})]^+$ ($Cp^* = \eta^5\text{-}C_5Me_5$), which have been known for 25 years remained limited [9]. The presence of five methyl substituents on the ancillary C_5-rings increases stability, solubility, and lowers oxidation potential, due to the amplified donor capacity of the Cp* ligand [10]. Taking advantage of these favorable stereoelectronic properties, Astruc and co-workers isolated and studied a number of oxidation states of redox cascades both in mono- [11] and bis-sandwich complexes [8], as well as a polycationic metallodendrimer with 24 $[Cp^*Fe(\eta^6\text{-}C_6H_5)]^+$ termini [12].

In the last few years, we have been interested in mono- and dinuclear dipolar hydrazone D–π–A type organometallic chromophores, in which the electron-withdrawing cationic organometallic fragment $[CpFe(\eta^6\text{-arene})]^+$ (A) is connected to a potent donating organic [13–15] or ferrocenyl [16–18] subunits (D) by the asymmetric –NR–N=CR– (R = H, Me) hydrazone conjugated bridge (π), and shown that in such D–π–A type systems an electronic cooperativity between the electron-donating and electron-accepting termini takes place through the entire hydrazone skeleton. Very recently, we used the powerful electron-withdrawing ability of this cationic mixed sandwich to prepare dipolar organometallic chromophores to achieve second-order nonlinear optical (NLO) responses [19]. However, the $CpFe(\eta^6\text{-arene})]^+$ salts are light sensitive, resulting in the decoordination of the $CpFe^+$ moiety [20], thus, in some instances, hampering NLO measurements [21]. To circumvent this problem, and at the same time prepare chromophores suitable for molecular materials with NLO properties, the $CpFe^+$ moiety has been substituted for its pentamethylated counterpart, thus generating an electron-withdrawing fragment, $[Cp^*Fe(\eta^6\text{-aryl})]^+$, which is stable under visible light irradiation [9,22]. The present contribution focuses on (i) the preparation and full spectroscopic characterization of two new organoiron(II) hydrazone D–π–A type systems using this pentamethylated cationic fragment as acceptor group, A, whereas the donor groups, D, are the mesityl groups, in the case of the mesitaldehyde hydrazone **4**, and the ferrocenyl unit, $CpFe(\eta^5\text{-}C_5H_4)$, in the case of the formylferrocene hydrazone **5**, the structural formulae of **4** and **5** are given in Scheme 3, (ii) their electrochemical behavior, and (iii) their nonlinear properties with the determination of μβ, by the electric-field-induced-second-harmonic (EFISH) generation technique. The crystal and molecular structure of the organometallic hydrazine precursor $[Cp^*Fe(\eta^6\text{-}C_6H_5)NHNH_2]^+PF_6^-$ (**3**), as well as the synthesis and characterization of the dicationic heterobimetallic hydrazone, $[Cp^*Fe\{\mu,\eta^6:\eta^6\text{-}(C_6H_5)\text{-}NHN{=}CH(2,4,6\text{-}Me_3C_6H_2)\}\text{-}RuCp^*]^{2+}(PF_6^-)_2$ (**6**), are also reported.

2. Results and discussion

2.1. Synthesis and characterization

We initially investigated ligand exchange reactions between $Cp^*Fe(CO)_2Br$ and *p*-dichlorobenzene in order to prepare the mixed sandwich $[Cp^*Fe(\eta^6\text{-}p\text{-}Cl_2C_6H_4)]^+PF_6^-$ (**1**). The dichlorobenzene has been chosen because in the final dipolar hydrazone product, the remaining electron-withdrawing chloro substituent should partly compensate the electron-donating ability of the Cp* ligand. One can then expect the $[Cp^*Fe(\eta^6\text{-}p\text{-}ClC_6H_4)]^+$ fragment to behave as a $[CpFe(\eta^6\text{-aryl})]^+$ unit in term of electron accepting capability. The ligand exchange reaction has been carried out under conditions analogous to those used for the synthesis of $[Cp^*Fe(\eta^6\text{-alkylarene})]^+$ complexes (Scheme 1) [9], taking into account the improved conditions reported by Pearson and Xiao in the preparation of the unsubstituted Cp counterpart [23]. Despite these experimental precautions, the yields remained surprisingly very low, reaching only 11% in the better case. The ^1H NMR spectrum of **1** showed two resonances at $\delta = 1.88$ and 6.32 ppm, assigned to the Cp* and arene protons, respectively, with relative intensity 15:4. The corresponding $^{13}C\{^1H\}$ NMR spectrum presented the four singlets attributed to the four different types of carbon nuclei. The cyclovoltammogram of **1** displayed two irreversible reduction waves at −1.74 and −1.87 V *vs.* $[Cp_2Fe]^{0/+}$, the more anodic one being attributable to a dechlorination reaction [24,25]. These redox potentials are indeed comparable to

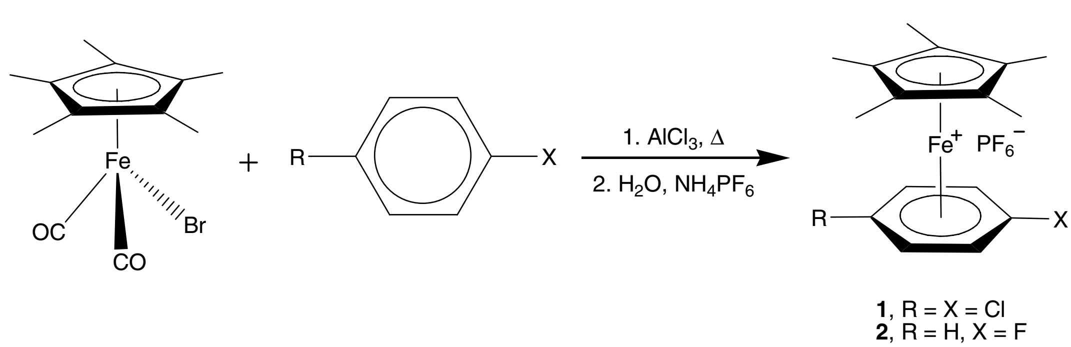

Scheme 1.

the −1.41 V/SCE reported for $[CpFe(\eta^6\text{-}C_6H_6)]^+$ [7,26]. This remains, however, a crude estimation of the electron-withdrawing ability.

As it became clear that compound **1** could not be used as a viable starting material, we turned our attention to the fluorobenzene mixed sandwich $[Cp^*Fe(\eta^6\text{-}C_6H_5F)]^+PF_6^-$ (**2**). It is easily accessible, followed a described procedure [27], by ligand substitution between $Cp^*Fe(CO)_2Br$ and the fluorobenzene in the presence of $AlCl_3$. This reaction was carried out at reflux of the fluorobenzene (85 °C) overnight (Scheme 1). Compound **2** was isolated in 26% yield as air and thermally stable green microcrystals. In the ^1H NMR spectrum of **2**, the characteristic sharp singlet of the Cp^* protons appeared at $\delta = 2.05$ ppm, a downfield shift presumably provoked by the presence of the electron-withdrawing fluorine atom onto the arene ring. The peculiar feature in the $^{13}C\{^1H\}$ spectrum is the three $J_{C\text{–}F}$ coupling constants of 269.0, 20.8, and 7.0 Hz between the ^{19}F nucleus and the *ipso*-, *ortho*-, and *meta*-^{13}C nuclei of the C_6-ring, respectively. Interestingly, for both compounds **1** and **2**, elemental and spectroscopic data (see Section 4) clearly indicate that no dehalogenation has taken place during the ligand exchange reactions [4,28,29].

The new ionic organometallic hydrazines $[Cp^*Fe(\eta^6\text{-}C_6H_5)NHNH_2]^+PF_6^-$ (**3**) was synthetized by reacting the fluoroarene precursor **2** with 12 equiv of hydrazine hydrate, $NH_2NH_2 \cdot H_2O$ (Scheme 2), according to the procedure we have reported for its unsubstituted Cp analogue [15]. Compound **3** was isolated in 60% yield as air and thermally stable yellow solid. Despite the decreased positive charge on the arene ligand compared to the Cp series, **3** is easily available by Cp^*Fe^+ induced nucleophilic aromatic substitution of the fluorobenzene [6]. No doubt that the excellent leaving group property of the fluoride ion favors this reaction.

The $–NHNH_2$ substituent was clearly identified in the IR spectrum of **3** with (i) two broad weak and medium absorption bands at 3417 and 3381 cm^{-1}attributed to the stretching mode of the N–H bond and to the asymmetric and symmetric stretching modes of the terminal NH_2 group, and (ii) with a sharp strong band at 1548 cm^{-1} corresponding to the deformation mode of the NH_2 group. In addition, the two intense vibration modes of the PF_6^- anion appeared at 839 and 558 cm^{-1}, respectively. In the ^1H NMR spectrum of **3**, the sharp singlet integrating for 15H at $\delta = 1.97$ ppm was unambiguously attributed to

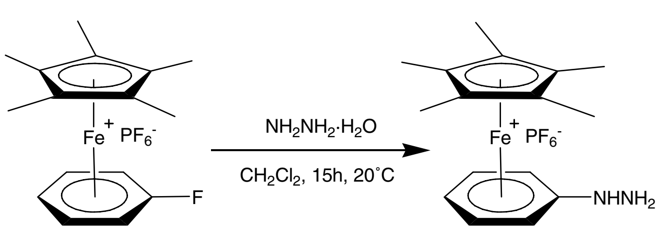

Scheme 2.

the Cp^* protons, indicating that the reaction went to completion. The $–NHNH_2$ group is clearly identified by the broad resonances at $\delta = 4.44$ and 7.35 ppm integrating for 2H and 1H, respectively. It is worth noting that the NH signal is upfield shifted by 1.40 ppm in **3** compared to its Cp counterpart, thus, nicely illustrating the increased electronic density onto the arene ring upon coordination to the Cp^*Fe^+ moiety. The $^{13}C\{^1H\}$ NMR spectrum showed all the expected signals with the carbon bearing the hydrazido group resonating at $\delta = 120.6$ ppm. A single crystal diffraction study also confirmed the proposed formulation (*vide infra*).

The new mono- and binuclear chromophores **4** and **5** were successfully prepared by a condensation reaction of the ionic organometallic hydrazine precursor $[Cp^*Fe(\eta^6\text{-}C_6H_5)NHNH_2]^+PF_6^-$ (**3**) with the mesitaldehyde and the ferrocenecarboxaldehyde, respectively, in ethanol solution (Scheme 3). The two complexes were isolated as orange microcrystalline solids, in 75% and 68% yields, respectively. Both the mono- and binuclear species display good thermal stability in air. Both **4** and **5** exhibit, in common polar organic solvents, a good solubility, but are insoluble in diethylether, hydrocarbons, and water. Their structures were inferred from satisfactory elemental analysis, NMR (^1H and ^{13}C), IR and UV–Vis spectroscopy.

In the solid-state IR spectra of compounds **4** and **5**, the ν(N–H) stretching vibrations of the terminal NH_2 group of precursor **3** have vanished, and they now exhibit the three typical features we have previously observed for mono- and binuclear organometallic hydrazones in the Cp series [13,18]. Those are: (i) a medium ν(N–H) stretching vibration at 3329 and 3322 cm^{-1} and (ii) a sharp intense band at 1558 and 1555 cm^{-1} attributed to the asymmetric ν(C=N) stretching vibration, for **4** and **5**, respectively, and (iii) two very strong $\nu(PF_6)$ ad δ(P–F) bands at 838 and 557cm^{-1}, respectively, for the two complexes.

As expected from previous work [13–18], both the mono- and binuclear organoiron hydrazones **4** and **5** are stereoselectively formed as the sterically less hindered *trans*-isomer (about the N=C double bond) as indicated by the unique set of signals in their ^1H and ^{13}C NMR spectra (see Section 4). The sandwich moiety $[Cp^*Fe(\eta^6\text{-}C_6H_5\text{–})]^+$ is clearly identified by the characteristic sharp singlet and the upfield multiplet of the Cp^* and phenyl proton resonances observed at δ *ca.* 2.0 and 5.9 ppm, respectively. The hydrazone spacer is characterized by the low field imine and acidic benzylic N–H protons which resonate at $\delta = 8.57$ and 8.03 ppm and 9.87 and 9.69 ppm for **4** and **5**, respectively. The latter signals are strongly upfield shifted compared to the N–H signal in **3** ($\delta = 7.35$ ppm), indicating depyramidalization of the nitrogen atom with partial delocalization of the positive charge and concommittent cyclohexadienyl character at the coordinated C_6-ring [13,18]. In addition, the peaks corresponding to the donor terminus protons, mesityl for **4** and ferrocenyl for **5**, appeared with the integral ratio 3:6:2 and 5:2:2, respectively.

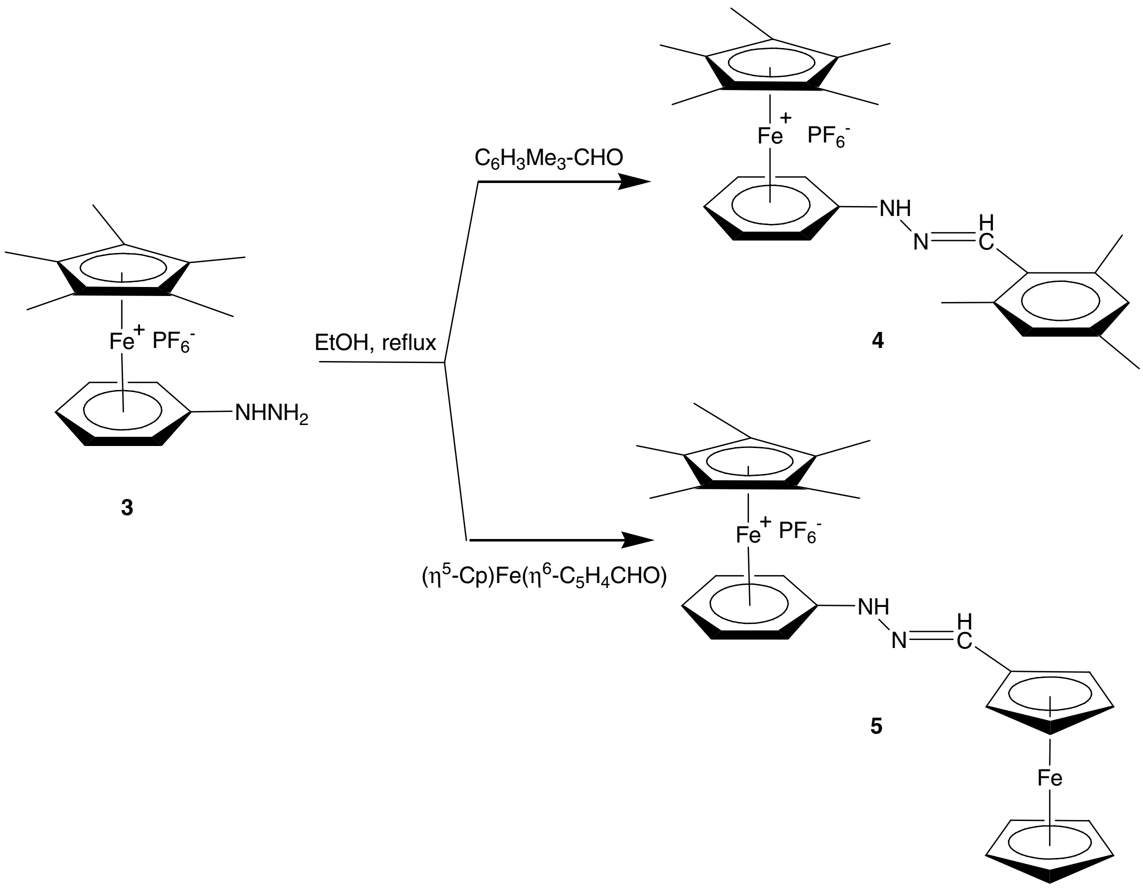

Scheme 3.

Consistent with the proposed structure, the ^{13}C NMR spectra of complexes **4** and **5** exhibited all the expected resonance signals. The two carbon atoms linked to a nitrogen atom appear at lower field, the imine carbon at *δ ca.* 145 and the coordinated C_{ipso} at *ca.* 120 ppm. For both complexes, this latter resonance splits into two peaks separated by 0.1 ppm. This could result from a possible equilibrium between a η^6-aminoarene and a η^5-iminocyclohexadienyl coordination modes to the Cp^*Fe^+ moiety, as supported by theoretical work [11] and previous solid-state studies [13–18,30]. In compound **4**, the carbon atoms of the coordinated C_6-ring are upfield shifted relative to those of the free mesityl ring.

Complexation of the mesityl ring in **4** by the Cp^*Ru^+ arenophile [31], followed by benzylic C–H bond activation [32] and subsequent bond formation, could lead to sophisticated molecules [33] incorporating the organoiron(II) hydrazones at the periphery. Accordingly, **4** was reacted with $[Cp^*Ru(NCCH_3)_3]^+PF_6^-$ overnight at room temperature followed by 2 h at reflux in CH_2Cl_2 to give the dicationic heterobimetallic complex **6** as an orange yellow solid in 59% yield (Scheme 4). Compound **6** is soluble in common polar organic solvents, and as a solid, is stable in air. This iron–ruthenium complex **6** represents the first example of a η^6:η^6-coordinated binucleating hydrazone ligand.

Compound **6** was characterized by elemental analysis and by standard spectroscopic techniques (see Section 4). As expected, the solid-state IR spectrum of **6** is essentially identical to those of **4** and **5**, with a weak *ν*(NH), a medium *ν*(C=N), and two very strong *ν*(PF_6) and *δ*(P–F) vibrations at 3325, 1559, 840, and 558 cm^{-1}, respectively. The assignment of the ^1H and ^{13}C NMR signals of **6** was performed with the aid of 2-D homo- and heteronuclear correlation spectroscopy. A comparison of the ^1H and ^{13}C NMR spectra of **4** and **6** clearly indicates the effect of the coordination of the Cp^*Ru^+ fragment to the mesityl ring. Whereas in the ^1H NMR spectrum of **4** the resonance signals of the methyl and aromatic protons appeared at 2.32, 2.56, and 7.00 ppm, in the ^1H NMR spectrum of **6** their corresponding signals are found at 2.29, 2.48, and 6.03 ppm, respectively. This upfield shift of the C_6-ring carbon signals is also observed in the ^{13}C NMR spectrum of **6**: $91.0 < \delta < 100.9$ ppm *vs.* $128.9 < \delta < 139.5$ for the free ligand in **4**. Such upfield ^1H and ^{13}C resonance shifts, as well as those observed above for **1**–**5**, have been reported for many other η^6-arene metal complexes and are explained by charge transfer between the arene and metal complex that results in a net reduction in C–C bond orders [34]. Another interesting feature of the presence of a second acceptor fragment in the molecule is the downfield shift of the benzylic N–H proton signal ($\delta = 10.19$ *vs.* 9.87 in **4**), as a consequence of the mutual electronic influence of the mixed sandwich termini through the conjugated hydrazone bridge.

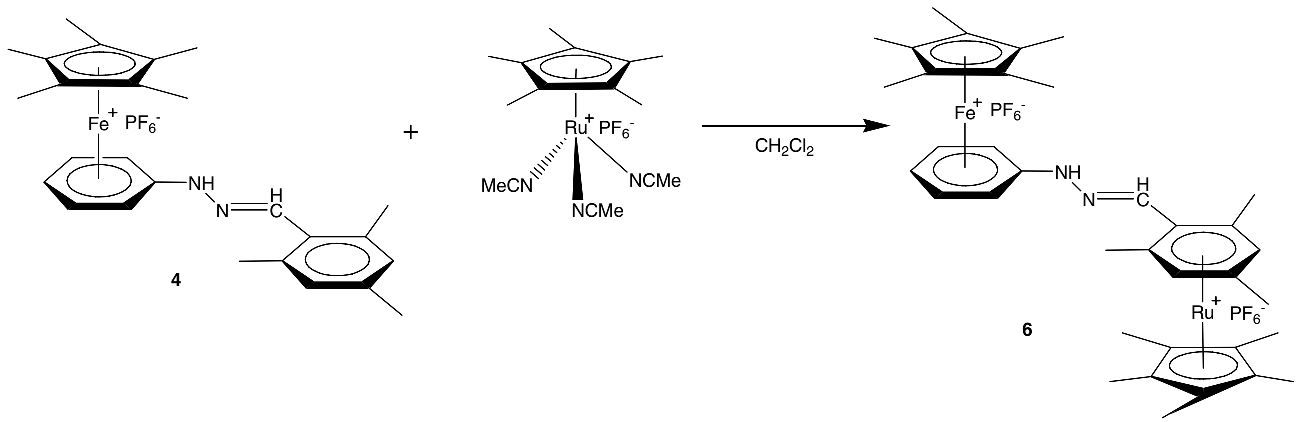

Scheme 4.

2.2. X-ray crystallographic studies

Single crystals of $[Cp^*Fe(\eta^6\text{-}C_6H_5)NHNH_2]^+PF_6^-$ (**3**) suitable for X-ray analysis were grown by slow diffusion of diethyl ether into a concentrated CH_2Cl_2 solution at room temperature. Data from the structural study are presented in Section 4.8, selected bond lengths for the cationic organometallic unit are presented in Table 1. An ORTEP view of the cation, with atom numbering, is shown in Fig. 1. Compound **3** crystallizes in the monoclinic space group $P2_1/n$ with four molecules in the unit cell. The iron atom is coordinated to the pentamethylcyclopentadienyl ring at a ring centroid-iron distance of 1.665 Å, and to the phenyl ring of the hydrazine ligand at a ring centroid-iron distance of 1.555 Å. The two carbocyclic rings are essentially parallel with one another, and the ring centroid-iron-ring centroid angle is of 179.4°. These metrical parameters together with those listed in Table 1 are very similar to those we have already reported for the parent compound $[CpFe(\eta^6\text{-}C_6H_5)NHNH_2]^+PF_6^-$ [15] and mononuclear organoiron(II) hydrazone complexes [13–15], and are typical of η^5-Fe-η^6 metallocene-type coordination [35].

On the other hand, one of the most remarkable deviation observed in the molecular parameters of complex **3** (Table 1) correspond to the Fe(1)–C(15) bond length, 2.194(3) Å, which is *ca.* 0.112 Å longer than the mean value of the other five Fe(1)–C(C_6-ring) bond lengths (2.082 Å). This elongation is a consequence of a partial delocalization of the benzylic nitrogen electron lone-pair toward the cationic mixed sandwich moiety, and is reflected by (i) a depyramidalization of the N(1) atom with idealized bond angles at this sp^2-hybridized nitrogen atom (C(15)–N(1)–N(2) = 118.1(2)°), (ii) a C(15)–N(1) bond length of 1.367(4) Å which is intermediate between a single and a double carbon–nitrogen bond [35], and (iii) a weak cyclohexadienyl character of the coordinated phenyl ring with a folding dihedral angle of 7.4° about the C(14)···C(16) axis. The substitution of the $CpFe^+$ for its pentamethylated analogue has virtually no effect on the deformation of the phenylhydrazine ligand toward an iminocyclohexadienyl structure. In the unsubstituted counterpart $[CpFe(\eta^6\text{-}C_6H_5)NHNH_2]^+PF_6^-$, the Fe–$C_{ipso}$ and C_{ipso}–N(1) are 2.146(6) and 1.333(9) Å, respectively, whereas the folding dihedral angle of the C_6-ring is 6.0(5)° [15]. The distortions of the arene ligand in hexahapto coordinated arene complexes are, indeed, mainly influenced by the electronegativity, the inductive and the resonance effects of the arene

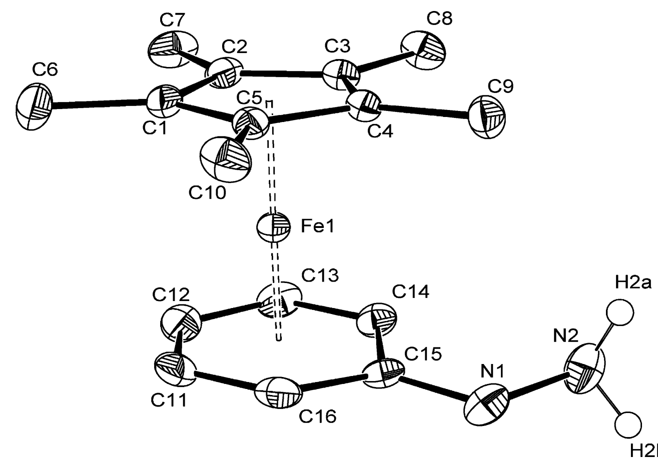

Fig. 1. Molecular structure and atom numbering scheme for **3**. Hydrogen atoms (except those of the NH_2 group) and the PF_6^- counterion have been omitted for clarity. Displacement ellipsoids are at the 50% probability level.

Table 1
Selected bond lengths (Å) and angles (°) for $[Cp^*Fe(\eta^6\text{-}C_6H_5)\text{-}NHNH_2]^+PF_6^-$ (**3**)

Distances			
Fe(1)–C(15)	2.194(3)	C(15)–N(1)	1.367(4)
Fe(1)–C(11-16)$_{av}$	2.082	N(1)–N(2)	1.413(4)
N(2)–H(2a)	0.88(4)	N(2)–H(2b)	0.85(4)
Fe(1)–Cp^*_{CNT}	1.665	Fe(1)–Ph_{CNT}	1.555
Angles			
C(15)–N(1)–N(2)	118.1(2)	C(14)–C(15)–C(16)	118.3(3)
N(1)–N(2)–H(2a)	112(3)	N(1)–N(2)–H(2b)	107(4)
H(2a)–N(2)–H(2b)	111(4)	Cp^*_{CNT}–Fe(1)–Ph_{CNT}	179.4

Abbreviations: $Cp^* = C_5(CH_3)_5$, Ph = C_6H_5, CNT = centroid.

Table 2
Electrochemical data[a] for **3–6**

Compounds	E_{pc} (V)[b]	$E_{1/2}$ (ΔE_p)[c] [V (mV)]	E_{pa} (V)[d]
3	−1.79	–	1.13
4	−1.78	–	1.18
5	−1.82	0.57 (78)	1.23
6	−1.91, −2.29	–	1.51, 1.71
Cp_2Fe	–	0.46 (70)	–

[a] Recorded in acetonitrile at 293 K with a vitreous carbon working electrode, with 0.1 M n-$Bu_4N^+PF_6^-$ as supporting electrolyte; all potentials are *vs.* Ag/AgCl; scan rate = 0.1 V/s.
[b] Peak potential of the irreversible wave corresponding to the reduction of the $[Cp^*Fe(\eta^6\text{-}C_6H_5)]^+$ fragment.
[c] Peak-to-peak separation between the resolved reduction and oxidation wave maxima.
[d] Peak potential of the irreversible wave corresponding to the oxidation of the $[Cp^*Fe(\eta^6\text{-}C_6H_5)]^+$ fragment.

substituents rather than by the nature of the 12-electron coordinating organometallic moiety ML_n [13–19,21,36–41].

2.3. Electrochemical studies

Cyclovoltammograms were recorded for the four complexes **3–6** at 20 °C in acetonitrile (see Section 4.1 for experimental details). Values of the reduction and oxidation potentials and information concerning the reversibilities are gathered in Table 2. The irreversible reduction wave of **3–5** and the first one of **6**, corresponds to the single-electron reduction of the d^6, Fe(II), 18-electron complexes to the unstable d^7, Fe(I), 19-electron species [7,9]. The redox potentials are in the expected range for pentamethylated iron sandwiches [7,9,11]. Interestingly, the peak potential of **5** is 40 mV more cathodic than that of **4**, which indicates that the electronic releasing effect of the ferrocenyl fragments on the sandwich iron center is somewhat greater than that of the mesityl subunit. Additionally, the cyclovoltammogram of compound **6** exhibited the irreversible reduction wave of the $[Cp^*Ru(\eta^6\text{-mesityl})]^+$ entity, at a very negative potential ($E_{pc} = -2.29$ V), more cathodic than that of the iron mixed sandwich terminus [42,43].

The compounds **3–5** show one irreversible oxidation wave in their cyclovoltammograms, whereas the heterobinuclear hydrazone **6** exhibits two irreversible oxidation processes, the most anodic one being attributed to the Ru(II)/Ru(III) couple [42,43]. The potential values listed in Table 2 are in agreement with those previously reported for methylated derivatives, $[Cp'Fe(\eta^6\text{-}C_6Me_{5-n}H_n NHR')]^+PF_6^-$ ($Cp' = Cp$, Cp^*; $R' = H$, n-Pr; $n = 0$, 4) [11]. The lowering of the oxidation potentials of **3–6** thus, the observation of the waves, results from the permethylation of the cyclopentadienyl ring. Such an oxidation wave has never been observed for any analogous organometallic hydrazones in the unsubstituted Cp series [13–18]. DFT calculations have shown that the HOMO of a complexed aniline has a large contribution from the HOMO of the free amine [11]. Therefore, it is likely that the oxidation of the complexes **3–6** involves removal of one electron from the HOMO which has also significant nitrogen lone-pair character.

Interestingly, complexation of the mesityl ring by the cationic arenophile Cp^*Ru^+ in **6** dramatically affects the oxidation potential of the iron sandwich center. The Fe(II)/Fe(III) couple is, indeed, anodically shifted by 330 mV on going from **4** to **6**. This suggests that a strong electronic interaction took place between the two metal centers through the entire hydrazone skeleton. This is also in line with the ^{1}H NMR observations (see above).

In the cyclovoltammogram of the homobimetallic hydrazone **5** (Fig. 2), the reversible one-electro oxidation process arises from the oxidation of the monosubstituted ferrocene unit and corresponds to the generation of the dicationic Fe(II)/Fe(III) mixed valence species. The E^0

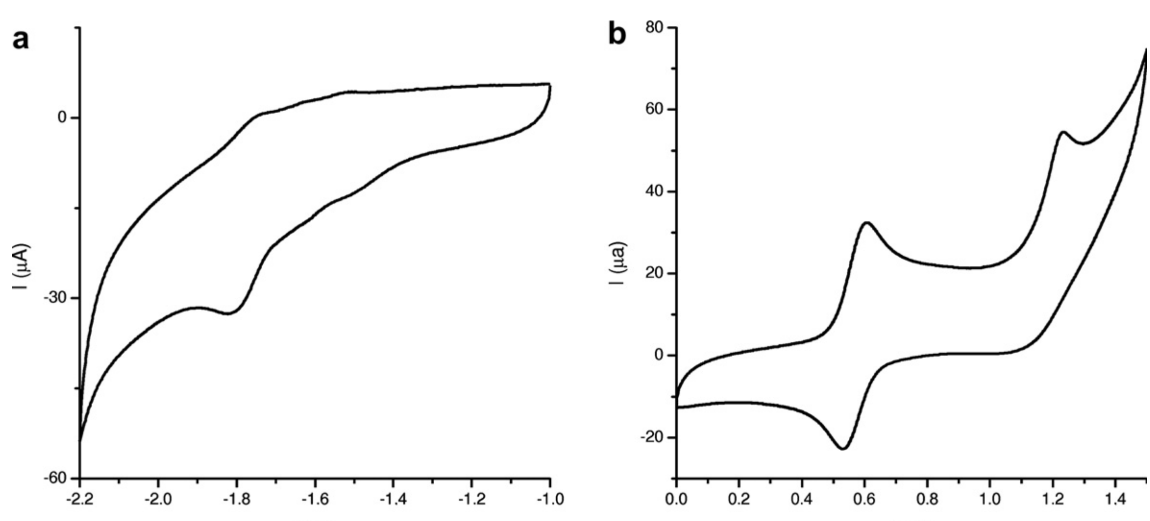

Fig. 2. Cyclic voltammograms of the homobimetallic hydrazone **5** recorded in MeCN/0.1 M n-$Bu_4N^+PF_6^-$ at $T = 293$ K and a voltage sweep rate v = 0.1 V/s, reference electrode Ag/AgCl, internal reference $Cp_2Fe^{0/+}$.

value is 110 mV positively shifted with respect to that of ferrocene (Table 2), thus featuring the electron-withdrawing properties of the pentamethylated cationic sandwich, $[Cp^*Fe(\eta^6-C_6H_5)]^+$. A more positive oxidation potential indicates that the ferrocenyl unit is more difficult to oxidize, *i.e.*, less electron rich. As expected, owing to the electron-donating effect of the five methyl substituents, this positive anodic shift is 50 mV weaker than that measured for the previously reported unsubstituted counterpart [18]. Finally, the electrochemical behavior of the homobimetallic hydrazone **5** is in agreement with the HOMO being essentially ferrocene based while the character of the LUMO is dominated by the cationic sandwich moiety, and fully consistent with theoretical results [18].

2.4. Linear and nonlinear optical properties

The UV–Vis spectra of complexes **3–6** are comparable in that the spectra consist of two intense broad absorption bands in the visible region (Fig. 3), indicating similar structural features. As expected, all the absorptions are blue-shifted upon permethylation of the C_5-ring. Indeed, the effect of the five electron-donating methyl groups consists in significant destabilization of the unoccupied π^* orbitals of the C_5-ring which are involved in the corresponding transitions. The origin of the high-energy absorption band in the range 300–350 nm, is assumed to be an intraligand charge-transfer (ILCT) transition, and the low-energy absorption band in the region 350–450 nm is assigned to a donor-to-acceptor charge transfer (DACT) transition [13,19,21,44]. From deconvolutions of the spectra with Gaussian curves, these two CT transitions give rise to two to four absorption bands (Table 3). The data of Table 3 indicate that linear optical properties (*i.e.*, energies and intensities of the absorption bands corresponding to the above-mentioned CT transitions) of **3–6** are in agreement with those reported for other D–π–A systems having the $[CpFe(\eta^6\text{-arene})]^+$ fragment as electron acceptor linked to an organic or organometallic electron-donating group [13–19,21]. The broadening of the low-energy band is probably the result of the overlap of broad d–d visible bands of the cationic sandwich fragment [9,45]. For the four compounds **3–6**, the two characteristic CT bands exhibit weak bathochromic shifts when the solvent polarity is increased, indicating increased polarity in the excited state. Note that the solvent influence is negligible for **5**, whereas a red shift of 23 nm and a hypsochromic shift of −24 nm are observed for the ILCT and DACT absorptions, respectively, for its nonmethylated counterpart [18].

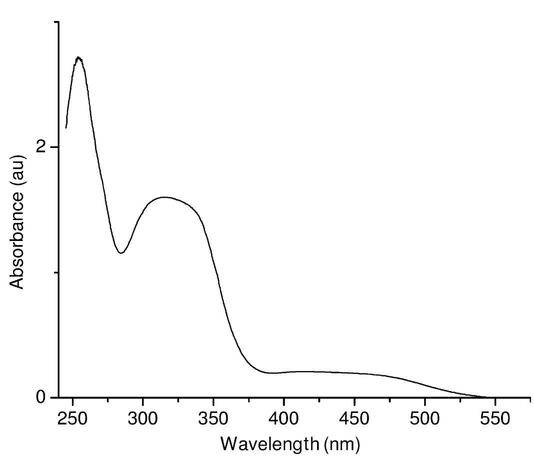

Fig. 3. UV–Vis spectrum of the homobimetallic complex hydrazone **5**.

Table 3
Electronic absorption and EFISH data

Compounds	λ/nm (Log ε)		Δλ/nm	$\mu\beta \times 10^{-8}$/esu
	CH_2Cl_2	DMSO		CH_2Cl_2
3	258 (4.36)			–
	322 (3.15)	334 (3.04)	+12	
	406 (2.47)	409 (2.40)	+3	
4	256 (4.34)			267 ± 20
	305 (4.24)	309 (4.24)	+4	
	342 (4.24)	347 (4.32)	+5	
	403 (3.22)	402 (3.40)	−1	
5	254 (4.38)			107 ± 20
	316 (4.15)	314 (4.12)	−2	
	412 (3.22)	412 (3.32)	0	
6	257 (4.47)			–
	298 (4.29)	300 (4.38)	+2	
	338 (4.30)	343 (4.44)	+5	
	402 (3.52)	406 (3.76)	+4	

The second-order NLO properties of compounds **4** and **5** have been investigated using the electric-field-induced-second-harmonic (EFISH) generation technique at 1.91 μm, which provides information about the scalar product μβ of the vectorial part of the first hyperpolarizability tensor β and the dipole moment vector μ [46–48]. Compounds **4** and **5** exhibited reasonable μβ values (Table 3). They are comparable to the 83, 149 and 154×10^{-48} esu values previously determined for three dipolar organoiron methylenepyran-hydrazone complexes ended with a similar cationic sandwich acceptor fragment [19]. However, the μβ values remain significantly weaker than those reported for extended π-conjugated organic hydrazone molecules ($\mu\beta = 100\text{–}640 \times 10^{-48}$ esu) bearing strong acceptor nitrophenyl end groups [49]. On the other hand, it is interesting to note that the μβ values of the homobimetallic complex **5** is more than half as large as that of the mononuclear derivative **4**. This weaker value may indicate a possible symmetrization of the conjugated electronic cloud over the whole molecule due to possible electronic transfer in the ground state from ferrocene to the cationic sandwich fragment (see Section 2.3). This symmetrization could explain the relatively lower μβ values for compound **5**, in spite of the presence of the ferrocenyl donor group.

Interestingly, it is noteworthy that, despite the increased electron donation upon substitution of the permethylated Cp ligands for its nonmethylated analogue, the cationic organoiron sandwich remains a strong electron acceptor terminus that could be used in molecular engineering for quadratic NLO.

3. Concluding remarks

In summary, the series of novel pentamethylated sandwich complexes based on the $[Cp^*Fe(\eta^6\text{-}C_6H_5)]^+$ core was obtained in good yields, except **1**, using well known reactions adapted to each case. Among them, two new organometallic π-conjugated push–pull chromophores **4** and **5** were prepared through condensations between the organometallic hydrazine precursor **3**, whose crystal structure has been determined by X-ray analysis, and either the mesitaldehyde or the ferrocenecarboxaldehyde, respectively. Their original design combines the cationic organometallic acceptor mixed sandwich, $[Cp^*Fe(\eta^6\text{-}C_6H_5)]^+$, associated with an organic or organometallic donor through the asymmetric hydrazone spacer –NH–N=CH–. Moreover, the mesityl unit of **4** is easily complexed by the arenophile Cp^*Ru^+, leading to the first η^6:η^6-coordinated dinucleating hydrazone. NMR and electrochemical data clearly indicate a mutual donor–acceptor electronic influence resulting from conjugation between the end groups through the entire hydrazone backbone. As such, the organometallic hydrazones **4** and **5** can be defined as Type I nonrod-shaped dipolar chromophores [50,51], and are proved to favor electronic delocalization along the conjugated chain. Finally, the first hyperpolarizability of the NLO properties of **4** and **5** have been measured by the EFISH technique. Interestingly, despite the increased electron donation brings about by the pentamethylation of the acceptor group, the μβ values are very similar to those determined for nonmethylated analogues [19]. However, the presence of two absorption bands in the visible region precludes analysis based only on a simple model, and theoretical investigations are needed to provide complementary information that would enable the interpretation of the UV–Vis spectra.

4. Experimental

4.1. General data

All operations were performed under inert atmosphere using standard vacuum/argon line, Schlenk or syringe techniques. Solvents were dried and distilled under argon by standard methods prior to use. $Cp^*Fe(CO)_2Br$ was prepared according to published procedure [9], and other chemicals were purchased from commercial sources and used without further purification. IR spectra were obtained with a Perkin Elmer Model 1600 FT-IR or a Bruker IFS28 FT spectrophotometers. Electronic spectra were collected on a Spectronic, Genesys 2, spectrophotometer. ^1H and ^{13}C NMR spectra were recorded in acetone-d_6 at 297 K on Bruker DPX 200, Advance 300 or Advance 500 instruments. All NMR spectra are reported in ppm (δ) relative to tetramethylsilane, with the residual solvent proton resonance and carbon resonances used as internal standards. Coupling constants (J) are reported in Hertz (Hz), and integrations are reported as number of protons. The following abbreviations are used to describe peak patterns: br = broad, s = singlet, d = doublet, t = triplet, m = multiplet. Electrochemical measurements were performed using a Radiometer Analytical model PGZ 100 All-in-one potentiostat, using a standard three-electrode setup with a vitreous carbon working and platinum wire auxiliary electrodes and a Ag/AgCl as the reference electrode. Solutions were 1.0 mM in the compound under study and 0.1 M in the supporting electrolyte $n\text{-}Bu_4N^+PF_6^-$. The ferrocene/ferricinium couple was used as an internal reference for the potential measurements. $E_{1/2}$ is defined as equal to $(E_{pa} + E_{pc})/2$, where E_{pa} and E_{pc} are the anodic and cathodic peak potentials, respectively. Melting points were determined in evacuated capillaries and were not corrected. Elemental analyses were conducted on a Thermo-FINNIGAN Flash EA 1112 CHNS/O analyzer by the Microanalytical Service of the Centre de Mesures Physiques de l'Ouest (CRMPO) at the University of Rennes 1, France.

4.2. Synthesis of $[Cp^*Fe(\eta^6\text{-}p\text{-}C_6H_4Cl_2)]^+PF_6^-$ (1)

A three necked round bottom flask equipped with a reflux condenser was purged with argon and charged with 4.0 g (12.2 mmol) of $Cp^*Fe(CO)_2Br$, 3.3 g (24.4 mmol) of $AlCl_3$, 30 g (0.2 mol) of *p*-dichlorobenzene and a magnetic stirbar. The reaction mixture was stirred and heated at 60 °C for 1 h, then 0.22 mL (12.2 mmol) of distilled water was added and the reaction mixture was heated overnight (15 h). The reaction mixture was cooled down to 40 °C, and the hydrolysis was carried out by careful addition of small portions of degassed ice-water. After phase separation, the aqueous solution was washed twice with 20 mL portion diethyl ether. Addition of aqueous NH_4OH, until pH 9 was reached, caused the precipitation of $Al(OH)_3$. The precipitate was filtered on a Büchner, washed several times with distilled water and the filtrate acidified with concentrated aqueous HCl until pH 7. Addition of an aqueous solution of NH_4PF_6 (1.99 g, 12.2 mmol) precipitated a yellow-green solid. This was filtered off, dissolved in acetone and dried over $MgSO_4$. After filtration, the solvent volume was reduced, and a green powder was precipitated after addition of diethyl ether. The solid was then filtered on a glass frit, washed with diethyl ether and dried under vacuum. Recrystallization from dichloromethane/diethyl ether provided compound **1** as light green microcrystals. Yield: 0.643 g (11%). Anal. Calc. for $C_{16}H_{19}Cl_2F_6FeP$ (483.0 g mol^{-1}): C, 39.78; H, 3.96. Found: C, 39.80; H, 3.72%. ^1H NMR (300.08 MHz): 1.88 (s, 15H, $C_5(CH_3)_5$), 6.32 (s, 4H, C_6H_4). $^{13}C\{^1H\}$ NMR (75.46 MHz): 8.29 (s, $C_5(CH_3)_5$), 89.26 (s, $C_5(CH_3)_5$), 94.11 (s, C_6H_4), 106.17 (s, C_6Cl_2). CV (Pt, CH_2Cl_2, $n\text{-}Bu_4NPF_6$, 20 °C, v = 0.1 V/s, E *vs.* $Cp_2Fe^{0/+}$): $E_{p1} = -1.74$ (irrev.), $E_{p2} = -1.87$ (irrev.).

4.3. Synthesis of $[Cp^*Fe(\eta^6\text{-}C_6H_5F)]^+PF_6^-$ (2) [27]

A three necked round bottom flask equipped with a reflux condenser was purged with argon and charged with

3.748 g (11.5 mmol) of $Cp^*Fe(CO)_2Br$, 6.10 g (45.6 mmol) of $AlCl_3$, 25 mL of fluorobenzene, and a magnetic stirbar. The reaction mixture was stirred and refluxed (85 °C) overnight (12 h). Workup as that described above for compound **1**, using in this case 1.874 g (11.5 mmol) of NH_4PF_6, afforded compound **2** as green microcrystals. Yield: 1.280 g (26%). Anal. Calc. for $C_{16}H_{20}F_7FeP$ (432.1 g mol^{-1}): C, 44.46; H, 4.86. Found: C, 44.39; H, 4.73%. IR(KBr, cm^{-1}): 3093w ν(CH arom), 2963w, 2922w, 2854w ν(CH aliph), 1232m ν(CF), 838vs ν(PF_6), 558s δ(P–F). ^{1}H NMR (200 MHz): 2.07 (s, 15H, $C_5(CH_3)_5$), 6.19–6.40 (m, 5H, C_6H_5). $^{13}C\{^1H\}$ NMR (50 MHz): 9.3 (s, $C_5(\mathit{C}H_3)_5$), 79.4 (d, o-C_6H_5, $^2J_{C-F}$ = 20.8 Hz), 88.9 (s, p-C_6H_5), 89.5 (d, m-C_6H_5, $^3J_{C-F}$ = 7.0 Hz), 92.9 (s,C_5 $(CH_3)_5$), 136.6 (d, C_{ipso}, $^1J_{C-F}$ = 269.0 Hz).

4.4. Synthesis of $[Cp^*Fe(\eta^6\text{-}C_6H_5NHNH_2)]^+PF_6^-$ (3)

A Schlenk tube was loaded with 220 mg (0.51 mmol) of compound **2**, 0.3 ml (6.17 mmol) of hydrazine hydrate ($N_2H_4 \cdot H_2O$), and 10 mL of CH_2Cl_2. The reaction mixture was stirred at room temperature for 15 h. Then, the solution was evaporated to dryness and the residue redissolved in CH_2Cl_2. A 5 mL aqueous solution of NH_4PF_6 (0.5 mmol) was added and the mixture was stirred and neutralized with 10% aqueous HCl. The product was recovered by extraction with CH_2Cl_2. The organic extract were combined and dried with $MgSO_4$. After filtration and upon removal of most of the CH_2Cl_2 by rotary evaporation, addition of diethyl ether precipitated the product, which was filtered off, washed with diethyl ether and dried under vacuum. Yield: 136 mg (60%) of yellow microcrystals. A crystal from this crop was used for an X-ray structure determination. Mp 236 °C (dec.). Anal. Calc. for $C_{16}H_{23}F_6FeN_2P$ (444.2 g mol^{-1}): C, 43.26; H, 5.22; N, 6.31. Found: C, 43.24; H, 5.13; N, 6.03%. IR (KBr, cm^{-1}): 3417w, 3381m ν(NH), 3091w ν(CH arom), 2963w, 2923w, 2855w ν(CH aliph), 1548s δ(NH_2), 839vs ν(PF_6), 558s δ(PF6). ^{1}H NMR (200 MHz): 1.97 (s, 15H, $C_5(CH_3)_5$), 4.44 (br s, 2H, NH_2), 5.55–5.77 (m, 5H, C_6H_5), 7.35 (s, 1H, NH). $^{13}C\{^1H\}$ NMR (50.3 MHz): 9.8 (s, $C_5(\mathit{C}H_3)_5$), 72.2 (s, o-C_6H_5), 85.5 (s, p-C_6H_5), 88.8 (s, $\mathit{C}_5(CH_3)_5$), 90.2 (s, m-C_6H_5), 120.6 (s, C_{ipso}).

4.5. Synthesis of $[Cp^*Fe(\eta^6\text{-}C_6H_5)\text{-}NHN{=}CH\text{-}(2,4,6\text{-}C_6H_2Me_3)]^+PF_6^-$ (4)

A Schlenk tube was charged with 112 mg (0.25 mmol) of compound **3**, 5 ml of ethanol, 0.1 mL (0.69 mmol) of mesitaldehyde, several drops of glacial acetic acid and a magnetic stirbar. The mixture was stirred and refluxed for 7 h. Then the reaction medium was cooled to room temperature. The orange solid formed was filtered off, washed twice with 5 mL portion diethyl ether and dried under vacuum. Yield: 107 mg (75%) of an orange powder. Mp 225 °C (dec.). Anal. Calc. for $C_{26}H_{33}F_6FeN_2P$ (574.4 g mol^{-1}): C, 54.36; H, 5.79; N, 4.88. Found: C, 54.19; H, 5.91; N, 4.84%. IR (KBr, cm^{-1}): 3329m ν(NH), 3094w ν(CH arom), 2965w, 2926w ν(CH aliph), 1558s ν(C=N), 838vs ν(PF_6), 557s δ(PF_6). ^{1}H NMR (200 MHz): 1.98 (s, 15H, $C_5(CH_3)_5$), 2.32 (s, 3H, 4-Me $C_6H_2Me_3$), 2.56 (s, 6H, 2,6-Me $C_6H_2Me_3$), 5.79–5.99 (m, 5H, C_6H_5), 7.00 (s, 2H, $C_6\mathit{H}_2Me_3$), 8.57 (br s, 1H, CH), 9.87 (s, 1H, NH). $^{13}C\{1H\}$ NMR (50.3 MHz): 9.9 (s, $C_5(\mathit{C}H_3)_5$), 21.1 (s, 4-Me $C_6H_2Me_3$), 22.1 (s, 2,6-Me $C_6H_2Me_3$), 71.74 and 71.78 (o-C_6H_5), 85.6 (s, p-C_6H_5), 88.9 (s, m-C_6H_5), 90.8 (s, $\mathit{C}_5(CH_3)_5$), 119.7 and 119.8 (C_{ipso}, C_6H_5), 128.9 (s, C_{ipso}, $C_6H_2Me_3$), 130.7 (s, 3,5-$C_6H_2Me_3$), 138.2 (s, 2,6-$C_6H_2Me_3$), 139.5 (s, 4-$C_6H_2Me_3$), 144.8 (s, =CH).

4.6. Synthesis of $[Cp^*Fe(\eta^6\text{-}C_6H_5)\text{-}NHN{=}CH\text{-}(\eta^5\text{-}C_5H_4)\text{-}Fe(\eta^5\text{-}C_5H_5)]^+PF_6^-$ (5)

A Schlenk tube was charged with 222 mg (0.50mmol) of compound **3**, 114 mg (0.53 mmol) of ferrocenecarboxaldehyde, 5 mL of ethanol, several drops of glacial acetic acid and a magnetic stirbar. The mixture was stirred and refluxed for 16 h. Workup as that described above for complex **4** provided compound **5** as an orange microcrystalline powder. Yield: 217 mg (68%); mp 197 °C (dec.). Anal. Calc. for $C_{27}H_{31}F_6Fe_2N_2P$ (640.2 g mol^{-1}): C, 50.64; H, 4.88; N, 4.37. Found: C, 50.31; H, 4.86; N, 4.12%. IR (KBr, cm^{-1}): 3322m ν(NH), 3094w ν(CH arom), 2963w, 2922w, 2855w ν(CH aliph), 1555s ν(C=N), 839vs ν(PF_6), 558s δ(PF_6). ^{1}H NMR (300.08 MHz): 1.97 (s, 15H, $C_5(CH_3)_5$), 4.25 (s, 5H, C_5H_5), 4.46 (t, 2H, $^3J_{H-H}$ = 1.8 Hz, C_5H_4), 4.73 (t, 2H, $^3J_{H-H}$ = 1.8 Hz, C_5H_4), 5.71-5.89 (m, 5H, C_6H_5), 8.03 (s, 1H, =CH), 9.69 (s, 1H, NH). $^{13}C\{^1H\}$ NMR (75.46 MHz): 10.0 (s, $C_5(\mathit{C}H_3)_5$), 68.2 (s, C_5H_4), 69.9 (s, C_5H_5), 71.0 (s, C_5H_4), 71.50 and 71.54 (o-C_6H_5), 80.6 (s, C_{ipso} C_5H_4), 85.4 (s, p-C_6H_5), 88.8 (s, m-C_6H_5), 90.7 (s, $\mathit{C}_5(CH_3)_5$), 119.8 and 119.9 (C_{ipso} C_6H_5), 145.2 (s, =CH).

4.7. Synthesis of $[Cp^*Fe(\eta^6\text{-}C_6H_5)\text{-}NHN{=}CH\text{-}(\eta^6\text{-}2,4,6\text{-}C_6H_2Me_3)RuCp^*]^{2+}[PF_6^-]_2$ (6)

A Schlenck tube was charged with 252 mg (0.5 mmol) of $[Cp^*Ru(NCMe)_3]^+PF_6^-$, 220 mg (0.5 mmol) of compound **4**, 20 mL of freshly distilled CH_2Cl_2, and a magnetic stirbar. The suspension was stirred overnight and then refluxed for 2 h. After cooling to room temperature, the solution was filtered by cannula and the product was precipitated with diethyl ether. The orange-yellow powder was recrystallized in a CH_2Cl_2/toluene mixture (1:1). Yield: 283 mg (59%); mp 176 °C (dec.). Anal. Calc. for $C_{36}H_{48}F_{12}FeN_2P_2Ru$ (955.64 g mol^{-1}): C, 45.25; H, 5.06; N, 2.93. Found: C, 44.90; H, 4.90; N, 2.98%. IR (KBr, cm^{-1}): 3325w ν(NH), 3097vw ν(CH arom), 2983w, 2915w ν(CH alif), 1559m ν(C=N), 840vs ν(PF_6), 558s δ(PF_6). ^{1}H NMR (500.13 MHz): 1.93, 1.95 (2 × s, 2 × 15H, $C_5(CH_3)_5$), 2.29 (s, 3H, 4-Me $C_6H_2Me_3$), 2.48 (s, 6H, 2,6-Me $C_6H_2Me_3$), 5.83 (t, 1H, $^3J_{H-H}$ = 5.7 Hz, p-C_6H_5), 5.87

(br s, 2H, o-C_6H_5), 5.99 (br t, 2H, m-C_6H_5), 6.03 (s, 2H, $C_6H_2Me_3$), 8.28 (br s, 1H, =CH), 10.19 (br s, 1H, NH). ^{13}C NMR (125.77 MHz): 8.94, 9.07 ($C_5(CH_3)_5$), 17.07 (4-Me $C_6H_2Me_3$), 17.79 (2,6-Me $C_6H_2Me_3$), 71.72 (o-C_6H_5), 85.48 (p-C_6H_5), 88.22 (m-C_6H_5), 90.37 ($C_5(CH_3)_5$), 91.05 (3,5-$C_6H_2Me_3$), 93.16 (C_{ipso} $C_6H_2Me_3$), 94.98 ($C_5(CH_3)_5$), 98.76 (2,6-$C_6H_2Me_3$), 100.92 (4-$C_6H_2Me_3$), 117.31 (C_{ipso} C_6H_5), 137.68 (=CH).

4.8. X-ray crystal structure determination of $[Cp^*Fe(\eta^6\text{-}C_6H_5)NHNH_2]^+PF_6^-$ (**3**)

A yellow prism of complex **3** having dimensions of $0.35 \times 0.25 \times 0.25$ mm was mounted with epoxy cement on the tip of a glass fiber in a random orientation. Data collection was performed at 110(2) K on a Kappa-CCD Enraf-Nonius diffractometer equipped with a bidimensional CCD detector, using graphite monochromated Mo Kα radiation ($\lambda = 0.71073$ Å). The cell parameters are obtained with Denzo and Scalepack [52] with 10 frames (psi rotation: 1° per frame). The data collection [53], $2\theta_{max} = 60°$, 1457 frames via 2.0° omega rotation and 7 s per frame, range HKL: H 0,8; K 0,22; L −20,20, gave 23913 reflections. The data reduction with Denzo and Scalepack [52] leads to 4158 independent reflections from which 3747 reflexions with $I > 2.0\sigma(I)$. Lorenz and polarization corrections were applied. The space groups was chosen based on the systematic absences in the diffraction data. The structure was solved using the direct method [54], completed by subsequent Fourier syntheses, and refined by full matrix least-squares procedures on reflection intensities (F^2) [55]. The absorption was not corrected. The positions of the hydrogen atoms of the terminal NH_2 group was determined from the electron difference map, and refined. All nonhydrogen atoms were refined anisotropically. Hydrogen atoms, with the exception noted, were placed in their calculated positions, assigned fixed isotropic thermal parameters and allowed to ride on their respective parent atoms. Atomic scattering factors were taken from the literature [56]. ORTEP views were generated with PLATON-98 [57].

4.8.1. Crystallographic data for **3**

$C_{16}H_{23}F_6FeN_2P$, $M_r = 444.18$ g mol^{-1}, monoclinic, $P2_1/n$, unit cell dimensions: $a = 6.8961(1)$, $b = 16.9749(3)$, $c = 15.5437(3)$ Å, $\beta = 91.4716(7)°$, $V = 1818.95(5)$ Å^3, $Z = 4$, $D_{calc} = 1.622$ g cm^{-3}, $\mu = 0.978$ mm^{-1}, $F(000) = 912$. Data/restraints/parameters: 4156/0/242, R/R_{w2} ($I > 2\sigma(I)$) = 0.0470/0.1186, R/R_{w2} (all data) = 0.0523/0.1226, GOF = 1.038, $[\Delta\rho]_{min}/[\Delta\rho]_{max}$: −0.730/1.186.

4.9. EFISH measurements

The principle of EFISH technique is described elsewhere [46,47]. In order to avoid reabsorption of the generated second harmonics, the data were recorded using 1.907 μm, 10 ns incident laser pulses produced by a hydrogen Raman shifter pumped by a Nd:YAG laser at 1.06 μm at a 10 Hz repetition rate. The centrosymmetry of the solution was broken by dipolar orientation of the chromophores with a high-voltage pulse (8 kV applied on 3 mm during 1 μs) synchronized with the laser pulse. The compounds were dissolved in dichloromethane at various concentrations (10^{-3}–10^{-2} mol l^{-1}) and the solutions were introduced into the measurement cell where the high-voltage was applied during SHG measurements. NLO measurements are calibrated with pure dichloromethane acting as a reference. Acquisition and data processing are performed using a computerized home-made system.

Acknowledgements

Thanks are expressed to P. Hamon and Dr. J. A. Shaw-Taberlet (Rennes) for generous gifts of pentamethylcyclopentadiene and $[Cp^*Ru(NCMe)_3]^+PF_6^-$ samples, respectively, to Dr. S. Sinbandhit (CRMPO, Rennes) for skillful assistance in recording high field NMR, and to Dr. J. Ruiz (Bordeaux) for providing preliminary NMR data of **2**. The authors also gratefully acknowledge Fondo Nacional de Desarrollo Científico y Tecnológico, FONDECYT (Chile), Grant No. 1010318 (D.C., C.M.), the Programme International de Coopération Scientifique, CNRS-CONICYT No. 18173 (C.M., D.C., J.-R.H.) for financial support.

Appendix A. Supplementary material

CCDC 603034 contains the supplementary crystallographic data for this paper. These data can be obtained free of charge via http://www.ccdc.cam.ac.uk/conts/retrieving.html, or from the Cambridge Crystallographic Data Centre, 12 Union Road, Cambridge CB2 1EZ, UK; fax: (+44) 1223-336-033; or e-mail: deposit@ccdc.cam.ac.uk. Supplementary data associated with this article can be found, in the online version, at doi:10.1016/j.jorganchem.2006.11.008.

References

[1] A. Togni, R.L. Halterman, Metallocenes, Wiley-VCH, 1998.
[2] N.J. Long, Metallocenes – An Introduction to Sandwich Complexes, Blackwell Scientific Publications, Oxford, 1998.
[3] A. Togni, T. Hayashi, Ferrocenes, VCH, Weinheim, Germany, 1995.
[4] D. Astruc, Top. Curr. Chem. 160 (1991) 47.
[5] A.S. Abd-El-Aziz, I. Manners, J. Inorg. Organomet. Polym. Mater 15 (2005) 157, and references therein.
[6] D. Astruc, S. Nlate, J. Ruiz, in: D. Astruc (Ed.), Modern Arene Chemistry: Concepts, Synthesis and Applications, Wiley-VCH, Weinheim, 2002, p. 400 (Chapter 12).
[7] D. Astruc, Electron Transfer and Radical Reactions in Transition-Metal Chemistry, VCH, New York, 1995, p. 147 (Chapter 2).
[8] D. Astruc, Acc. Chem. Res. 30 (1997) 383, and references therein.
[9] J.-R. Hamon, D. Astruc, P. Michaud, J. Am. Chem. Soc. 103 (1981) 758.
[10] R.H. Crabtree, The Organometallic Chemistry of the Transition Metals, third ed., Wiley-VCH, New York, 2001.

[11] J. Ruiz, F. Ogliaro, J.-Y. Saillard, J.-F. Halet, F. Varret, D. Astruc, J. Am. Chem. Soc. 120 (1998) 11693.
[12] C. Valério, E. Alonso, J. Ruiz, J.-C. Blais, D. Astruc, Angew. Chem., Int. Ed. 38 (1999) 1747.
[13] C. Manzur, L. Millán, W. Figueroa, D. Boys, J.-R. Hamon, D. Carrillo, Organometallics 22 (2003) 153.
[14] C. Manzur, L. Millán, W. Figueroa, J.-R. Hamon, J.A. Mata, D. Carrillo, Bol. Soc. Chil. Quim. 47 (2002) 431.
[15] C. Manzur, E. Baeza, L. Millán, M. Fuentealba, P. Hamon, J.-R. Hamon, D. Boys, D. Carrillo, J. Organomet. Chem. 608 (2000) 126.
[16] C. Manzur, L. Millán, M. Fuentealba, J.A. Mata, D. Carrillo, J.-R. Hamon, J. Organomet. Chem. 690 (2005) 1265.
[17] C. Manzur, C. Zúñiga, L. Millán, M. Fuentealba, J.A. Mata, J.-R. Hamon, D. Carrillo, New J. Chem. 28 (2004) 134.
[18] C. Manzur, M. Fuentealba, L. Millán, F. Gajardo, D. Carrillo, J.A. Mata, S. Sinbandhit, P. Hamon, J.-R. Hamon, S. Kahlal, J.-Y. Saillard, New J. Chem. 26 (2002) 213.
[19] L. Millán, M. Fuentealba, C. Manzur, D. Carrillo, N. Faux, B. Caro, F. Robin-Le Guen, S. Sinbandhit, I. Ledoux-Rak, J.-R. Hamon, Eur. J. Inorg. Chem. (2006) 1131.
[20] J.-R. Hamon, J.-Y. Saillard, A. Le Beuze, M.J. McGlinchey, D. Astruc, J. Am. Chem. Soc. 104 (1982) 7549.
[21] C. Lambert, W. Gaschler, M. Zabel, R. Matschiner, R. Wortmann, J. Organomet. Chem. 592 (1999) 109.
[22] J.L. Schrenk, A. McNair, F.B. McCormick, K.R. Mann, Inorg. Chem. 25 (1986) 3501.
[23] A.J. Pearson, W.J. Xiao, J. Org. Chem. 68 (2003) 2161.
[24] This fully irreversible wave could be attributed to the 2-electron reduction of the C–Cl functionality, following the ECE mechanism for the reduction of Ar–X into Ar^- and X^- [25]. Its integrated area is twice that of the wave at −1.87 V, ascribed to the in situ generated $[Cp^*Fe(\eta^6\text{-}ClC_6H_5)]^+PF_6^-$.
[25] D.G. Peters, Organic electrochemistry, in: H. Lund, O. Hammerich (Eds.), Halogenated Organic Compounds, 4th ed., Marcel Dekker, New York, 2001, p. 341 (Chapter 8).
[26] R.E. Dessy, F.E. Stary, R.B. King, M. Waldrop, J. Am. Chem. Soc. 88 (1966) 471.
[27] This compound was originally prepared and employed by Astruc and co-workers to built Polycationic Metallodendrimers but its analytical and spectroscopic characterizations were never reported; (a) C. Valério, Ph.D. Dissertation, Université Bordeaux I, 1996; (b) See Ref. [12].
[28] A.N. Nesmeyanov, N.A. Vol'kenau, I.N. Bolesova, Tetrahedron Lett. (1963) 1765.
[29] I.U. Khand, P.L. Pauson, W.E. Watts, J. Chem. Soc. C (1968) 2257.
[30] W. Figueroa, M. Fuentealba, C. Manzur, D. Carrillo, A.I. Vega, J.-Y. Saillard, J.-R. Hamon, Organometallics 23 (2004) 2515.
[31] P.J. Fagan, M.D. Ward, J.C. Calabrese, J. Am. Chem. Soc. 111 (1989) 1698.
[32] M.C. Casado, T. Wagner, D. Astruc, J. Organomet. Chem. 502 (1995) 143.
[33] B. Alonso, J.-C. Blais, D. Astruc, Organometallics 21 (2002) 1001.
[34] S.M. Hubig, S.V. Lindeman, J.K. Kochi, Coord. Chem. Rev. 200–202 (2000) 831.
[35] For a reference gathering a large number of interatomic and metal–ligand distances obtained from the Cambridge Crystallographic Data Base Centre, see: A.G. Orpen, L. Brammer, F.H. Allen, D. Kennard, D.G. Watson, R. Taylor, J. Chem. Soc., Dalton Trans. (1989) S1.
[36] Y. Ishii, M. Kawaguchi, Y. Ishino, T. Aoki, M. Hidai, Organometallics 13 (1994) 5062.
[37] S. Marcen, M.V. Jiménez, I.T. Dobrinovich, F.J. Lahoz, L.A. Oro, J. Ruiz, D. Astruc, Organometallics 21 (2002) 326.
[38] J.-Y. Saillard, D. Grandjean, P. Le Maux, G. Jaouen, Nouv. J. Chim. 5 (1981) 153.
[39] A. Moriuchi, K. Uchida, A. Inagaki, M. Akita, Organometallics 24 (2005) 6382.
[40] A.D. Hunter, L. Shilliday, W.S. Furey, M.J. Zaworotko, Organometallics 11 (1992) 1550.
[41] J.-P. Djukic, F. Rose-Munch, E. Rose, J. Vaissermann, Eur. J. Inorg. Chem. (2000) 1295.
[42] O.V. Gusev, M.A. Levlev, M.G. Peterleitner, S.M. Peregudova, L.I. Denisovich, P.V. Petrovskii, N.A. Ustynyuk, Russ. Chem. Bull. 45 (1996) 1601.
[43] O.V. Gusev, M.A. Ievlev, M.G. Peterleitner, S.M. Peregudova, L.I. Denisovich, P.V. Petrovskii, N. A Ustynyuk, J. Organomet. Chem. 534 (1997) 57.
[44] A. Le Beuze, R. Lissillour, J. Weber, Organometallics 12 (1993) 47.
[45] A.M. McNair, K.R. Mann, Inorg. Chem. 25 (1986) 2519.
[46] J.L. Oudar, D.S. Chemla, J. Chem. Phys. 66 (1977) 2664.
[47] J.L. Oudar, J. Chem. Phys. 67 (1977) 446.
[48] J.L. Oudar, H. Le Person, Opt. Commun. 15 (1975) 258.
[49] J. Zyss, I. Ledoux, J.-F. Nicoud, in: D.S. Chemla, J. Zyss (Eds.), Advances in Molecular Engineering for quadratic nonlinear optics, Molecular Nonlinear Optics, Academic Press, San Diego, 1994, p. 129.
[50] C. Serbutoviez, C. Bosshard, G. Knöpfle, P. Weiss, P. Prêtre, P. Günter, K. Schenk, E. Solari, G. Chapuis, Chem. Mater. 7 (1995) 1198.
[51] M.S. Wong, U. Meier, F. Pan, V. Gramlich, C. Bosshard, P. Günter, Adv. Mater. 8 (1996) 416.
[52] Z. Otwinowski, W. Minor, Processing of X-ray diffraction data collected in oscillation mode, in: C.W. Carter, R.M. Sweet (Eds.), Macromolecular Crystallography, Part A, Methods in Enzymology, vol. 276, Academic Press, London, 1997, p. 307.
[53] Nonius KappaCCD Software, Nonius B.V., Delft, The Netherlands, 1999.
[54] A. Altomare, M.C. Burla, M. Camalli, G.L. Cascarano, C. Giacovazzo, A. Guagliardi, A.G.G. Moliterni, G. Polidori, R. Spagn, J. Appl. Crystallogr. 32 (1999) 115.
[55] G.M. Sheldrick, SHELX97. Program for the Refinement of Crystal Structures, University of Göttingen, Göttingen, Germany, 1997.
[56] A.J.C. Wilson (Ed.), International Tables for X-ray Crystallography, vol. C, Kluwer Academic Publishers, Dordrecht, The Netherlands, 1992.
[57] A.L. Spek, PLATON-98, A Multipurpose Crystallographic Tool, Utrecht University, Utrecht, The Netherlands, 1998.